Catalysis Communications 61 (2015) 44–47

Contents lists available at ScienceDirect

Catalysis Communications

journal homepage: www.elsevier.com/locate/catcom

Short communication

Silver decorated alpha-manganese oxide nanostructured electrocatalyst for rechargeable lithium–oxygen battery

Zheng Huang [a,b], Ming Zhang [a], Junfang Cheng [a], Yingpeng Gong [a], Bo Chi [a,*], Jian Pu [a], Li Jian [a]

[a] Center for Fuel Cell Innovation, State Key Laboratory of Material Processing and Die & Mould Technology, School of Materials Science and Engineering, Huazhong University of Science & Technology, Wuhan 430074, China

[b] Research Center for Engineering Technology of Polymeric Composites of Shanxi Province, School of Materials Science and Engineering, North University of China, TaiYuan 030051, China

ARTICLE INFO

Article history:
Received 14 October 2014
Received in revised form 6 December 2014
Accepted 9 December 2014
Available online 11 December 2014

Keywords:
Silver
Alpha-MnO_2
Nano-electrocatalyst
Air electrode
Li–O_2 battery

ABSTRACT

Ag decorated α-MnO_2 nanorods are studied as a cathode catalyst for rechargeable lithium–oxygen battery (LOB). The composites are synthesized by in-situ composite technique in the presence of polymeric additives and characterized by SEM, XPS, and FT-IR. The battery with Ag decorated α-MnO_2 nanorod composite electrode shows an initial discharge capacity of 793 mA $hg^{-1}{}_{(electrode)}$, with reversible charge capacity of 778 mA $hg^{-1}{}_{(electrode)}$, while battery with only α-MnO_2 has discharge capacity of 510 mA $hg^{-1}{}_{(electrode)}$ and charge capacity of 504 mA $hg^{-1}{}_{(electrode)}$. No Li_2O or Li_2O_2 can be detected after discharge and Li_2CO_3 is the main discharge product, which suggests that the decomposition of organic carbonate electrolyte occurs during discharge.

1. Introduction

Rechargeable LOBs having the potential to provide 3–5 times gravimetric energy density of conventional Li-ion batteries [1,2] are very attractive for the future energy storage system. However, the development of LOBs faces a lot of challenges, such as low round-trip efficiency, low rate capability, poor cycle life and electrolyte instability [3]. The cathode is the bottle-neck of a nonaqueous LOB, wherein the terribly sluggish oxygen reduction/evolution reaction (ORR/OER) kinetics not only increases the overpotential, but also causes poor rechargeability and low rate capability [4]. Therefore, it is vital to develop highly effective catalyst. Until now, Pt and its alloys have been considered as the best catalysts for metal-oxygen batteries [5,6]. However, Pt remains an expensive metal of low abundance. Therefore, much of the focus has moved toward metal oxides [7], metal nitrides [8], phthalocyanine compounds [9], etc.

Manganese oxides (MnO_x) have been widely studied as an alternative to noble metal based catalysts because of their advantages, as abundance, low cost, environmental friendliness, and favorable ORR and OER activity [10,11]. Recently, Su et al. [12] reported that Mn ion oxidation state in MnO_x significantly influenced the catalytic activity for oxygen reduction and oxidation catalysis by using a combination of computational modeling and experiments. Mn shows oxidation states from +2 to +3 to +4 near the equilibrium potential for ORR and OER, suggesting that Mn can exchange oxygen atoms with the electrolyte at relevant potentials property which could potentially facilitate ORR and OER. Among various MnO_x polymorphs, α-MnO_2 is believed to be a promising catalyst. Higher activity of α-MnO_2 is attributed to the 2×2 tunnel frame structure and large number of defects [13]. Nevertheless, it is evident that the activity of α-MnO_2 still falls below those of noble metal-based catalysts [14,15].

Because of the excellent electronic conductivity of Ag, it would be an ideal conductor to form electron-transferring channels during manganese dioxide discharging. Ag can facilitate the direct reduction of O_2 to O^{2-}. The oxygen atoms that are not reduced to O^{2-} in the $4e^-$ process may be reduced to O_2^{2-} in a two electrons process. So, the combination of these two catalysts should significantly enhance the performance of the air electrode. Wu et al. [16] prepared Ag–MnO_x/C composites using $AgNO_3$ and $KMnO_4$ as the precursors and Vulcan XC-72 as the support. The Ag–MnO_x/C-300 shows the highest activity toward the ORR, with the half-wave potential of the ORR shifting negatively only 0.035 V compared to that on the commercial 40 wt.% Pt/C. The maximum power density of the zinc–air battery with the Ag–MnO_x/C-300 air electrode reaches up to 130 mW cm^{-2}, higher than those based on the Pd/C and Pt/C cathode catalysts.

Herein, we report Ag decorated α-MnO_2 nanostructured composite catalyst for rechargeable LOB. In such a composite structure, α-MnO_2 nanorods provide accessibility of active species during discharge and charge. Ag has comparable catalytic activity with Pt and Au, though its cost is much lower. Thus high activity is expected with the nanostructured composite cathode for LOB.

---

* Corresponding author.
E-mail address: chibo@hust.edu.cn (B. Chi).

http://dx.doi.org/10.1016/j.catcom.2014.12.009
1566-7367/© 2014 Elsevier B.V. All rights reserved.

2. Experimental

2.1. Synthesis

Chemical reagents were purchased from Beijing Chemical Works and used without further purification. In all processes ethanol (AR) and deionized water were used. In brief, 0.1 mol $KMnO_4$ and 0.15 mol $MnSO_4 \cdot H_2O$ were dissolved in 30 mL of deionized water separately. Then the $MnSO_4 \cdot H_2O$ solution was added to $KMnO_4$ solution slowly under magnetic stirring for 4 h. The solution was transferred into a 100 mL Teflon-line stainless steel autoclave and heated at 160 °C for 24 h. The products (α-MnO_2) were collected by centrifugation, washed with deionized water and dried under vacuum at 80 °C. 3.5 g $AgNO_3$ was dissolved in 60 mL deionized water, then 0.1 M $NH_3 \cdot H_2O$ (28 wt.%) was added until the solution became transparent again to form $[Ag(NH_3)_2]^+$ solution. Reducing solution was prepared by mixing 45 g $C_6H_{12}O_6$, 1.5 g PVP, 100 mL ethanol and 1 L deionized water together. 0.5 g α-MnO_2 was dispersed in 50 mL of 1 wt.% sodium dodecyl sulfonate (SDS) of $[Ag(NH_3)_2]^+$ solution for 30 min. Then α-MnO_2 with Ag nanoparticles can be obtained by mixing $[Ag(NH_3)_2]^+$ solution and reducing solution with a ratio of 1/1 (v/v) dropwise under magnetic stirring for 6 h. The final products were collected by centrifugation, washed with ethanol and dried under vacuum at 80 °C.

2.2. Measurement and characterization

The morphology and composition were investigated using a field emission scanning electron microscope (FE-SEM, FEI, Sirion 200) and X-ray photoelectron spectroscopy (XPS, ESCA-LAB 250 photoelectron spectrometer). FT-IR measurement was performed with a transmission method using KBr windows and mercury cadmium telluride (MCT) semiconductor detector was used.

Discharge–charge (DC) performance was carried out in a Hantest cycler (Wuhan Hantest Technology Co., Ltd.) with a lower voltage limit of 2.0 V and an upper limit of 4.0 V vs Li^+/Li under different current densities. The observed capacity was normalized by the total weight of the air electrode in this study. Before test, the batteries (detailed assembly processes are given in ESI) were rested for 4 h to reach equilibrium of oxygen concentrations and moisture of electrolyte.

3. Results and discussion

The morphology of α-MnO_2 with and without Ag particles decorating was analyzed by FESEM, as shown in Fig. 1. Fig. 1a confirms that the as-prepared α-MnO_2 is nanorod with a length of a few microns and diameter less than 100 nm. The nanorods have uniformity and good dispersion. Fig. 1b shows Ag decorated α-MnO_2 nanorods. It can be found that Ag snow crystals are homogeneously covering on the surface of nanorods, which is consistent with the XRD (Fig. S1) and EDS results (Fig. S2).

The chemical composition of Ag/α-MnO_2 catalyst was examined by XPS. Fig. 2 shows Ag 3d and Mn 2p regions of XPS spectra of the composite. In Fig. 2a, peaks of binding energy (BE) at 368.46 eV and 374.44 eV can be assigned to Ag $3d_{5/2}$ and Ag $3d_{3/2}$, which are similar to the metallic Ag with the characteristic peaks at 368 eV ($3d_{5/2}$) and 374 eV ($3d_{3/2}$) [17]. Besides that, the Mn 2p XPS spectrum exhibits two major peaks with BE values at 642.2 eV and 653.8 eV in Fig. 2b and a spin-energy separation of 11.6 eV, which are in good agreement with the reported data of Mn $2p_{3/2}$ and $2p_{1/2}$ for MnO_2 [18]. XPS results show that the composite consists of MnO_2 and Ag.

Fig. 3a is the typical discharge–charge curves of the LOB at 0.02 mA cm^{-2} using α-MnO_2, Ag/α-MnO_2 nanocomposite and physically mixed Ag–MnO_2 as cathode, respectively. Pure α-MnO_2 nanorods show an initial discharge capacity of 522 mA $hg^{-1}{}_{(electrode)}$ during the first cycle and the charge capacity of 507 mA $hg^{-1}{}_{(electrode)}$. The discharge plateau curve is flat at 2.8–2.9 V, which is comparable to reported data [19] and the charge potential plateau curve is observed at 3.9 V, which is slightly higher than the theoretical potential of 2.95 V vs. Li/Li^+. However, for Ag/α-MnO_2 nanocomposite cathode, the overall performance enhancement can be observed, compared with pure α-MnO_2 nanorod cathode. The open-circuit voltage (OCV) of the battery is about 3.15 ± 0.18 V, and the discharge plateau is large and flat at 2.84 V vs. Li/Li^+, which is close to the theoretical value of 2.95 V vs. Li/Li^+ for Li_2O_2 formation. The charge potential is also suppressed at 3.8 V vs. Li/Li^+ and shows a flat plateau curve with reversible capacity. It shows an initial discharge capacity of 944 mA $hg^{-1}{}_{(electrode)}$ with reversible charge capacity of 892 mA $hg^{-1}{}_{(electrode)}$ in Ag/α-MnO_2 nanocomposite cathode. It can also be found that physically mixed Ag and α-MnO_2 shows performance between the other two cathodes.

To further measuring the performance of the battery with Ag/α-MnO_2 nanocomposite cathode, the initial charge–discharge curves of the battery at 0.02, 0.05, and 0.1 mA cm^{-2} are shown in Fig. 3b. For comparison, A. K. Thapa et al. [20] reported LOB with a capacity of 817 mA $hg^{-1}{}_{(electrode)}$ using Pd/β-MnO_2 catalyst at 0.025 mA cm^{-2} and the battery exhibited stable specific capacities. Ex-situ and in-situ XRD results suggested that the observed capacity comes primarily from the oxidation of Li^+ to Li_2O_2 followed by Li_2O after discharge to 2.0 V vs Li/Li^+. However, the specific capacity and operating voltage of the battery with Ag/α-MnO_2 nanocomposite cathode decrease with

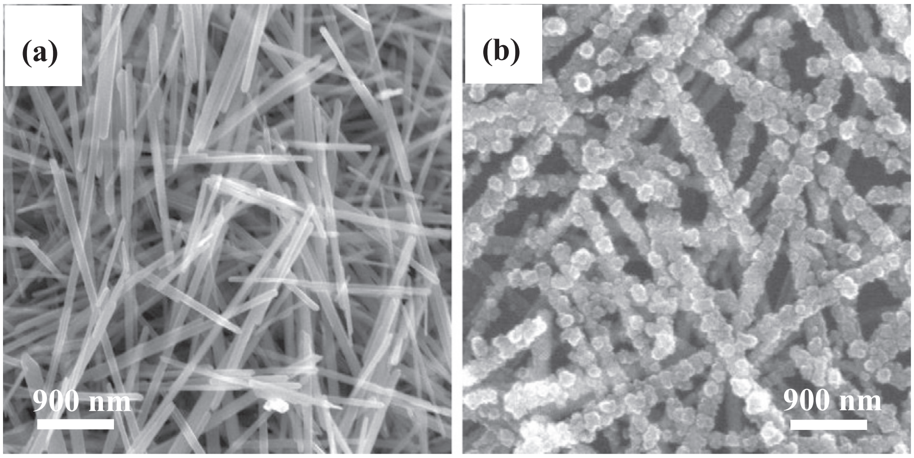

Fig. 1. Morphology of α-MnO_2 with and without Ag decorating. (a) pure α-MnO_2; (b) Ag decorated α-MnO_2.